

ATTENUATION OF PEAK GROUND MOTION  
AND ABSOLUTE ACCELERATION RESPONSE SPECTRA

by

Kazuhiko Kawashima<sup>I</sup>, Koh Aizawa<sup>II</sup> and Kazuyuki Takahashi<sup>II</sup>  
Presenting Author: K. Kawashima

SUMMARY

This paper presents the result of multiple regression analysis of 394 horizontal strong motion acceleration records obtained at 67 free field sites in Japan from 90 earthquakes with focal depth less than 60 km. Because sensitivity of the Japanese SMAC accelerograph is appreciably low at the high frequency range, instrumental correction was performed on the original data. Each pair of two orthogonal horizontal components was combined in time domain to get the maximum peak ground motions in the horizontal plane. The same composition was considered to get the maximum value of absolute acceleration response spectra with damping of 5% of critical on the horizontal plane. The records were classified into three groups due to subsoil condition. Empirical formulae of attenuation of the maximum peak ground motion (acceleration, velocity and displacement) and absolute acceleration response spectra with 5% damping ratio are proposed for three subsoil conditions.

INTRODUCTION

For determining appropriate seismic effects to be considered in design of structures, it is essential to assess intensities and frequency characteristics of severe ground motions. One of the characteristics of earthquake ground motions of considerable interest in design are the peak values of horizontal ground motions, i.e., peak ground acceleration, velocity and displacement. Earthquake response spectra, as defined by the maximum response of a single degree of freedom system, may be more relevant parameters to represent the characteristics of ground shaking because they account for both frequency characteristics and intensities of ground motion.

In this paper, multiple regression analyses were done on peak horizontal motions (acceleration, velocity and displacement) and absolute acceleration response spectra with 5% damping of critical. Attenuations of these characteristics in terms of earthquake magnitude and epicentral distance are proposed for three subsoil conditions.

STRONG MOTION DATA ANALYZED

A total of 197 sets of two horizontal components of strong motion accelerations were used in the analysis. They were recorded at 67 free field sites in Japan (Ref.1), and any records on structures including the first floor and basement were excluded. Only earthquakes with magnitude (JMA magnitude) greater than or equal to 5.0 and with focal depth less than 60 km were considered in analysis. The ground conditions at recording sites

- 
- I. Chief Research Engineer, Ground Vibration Division, Earthquake Disaster Prevention Department, Public Works Research Institute, Ministry of Construction, Tsukuba Science City, Ibaraki-ken, Japan  
II. Assistant Research Engineer, do

were classified into three groups as shown in Table 1. This classification essentially depends on Japanese practice adopted in the Earthquake Resistant Design Specifications of Highway Bridges (ERDSHB). A slight modification was, however, added to the ERDSHB classification, i.e., the original classification of ERDSHB has four categories for soil conditions, whereas three conditions were considered in this analysis by putting group 2 and 3 of ERDSHB classification into the same group.

All the data analyzed were provided by SMAC accelerograph. Because sensitivity at high frequency is substantially low in SMAC accelerograph, instrumental correction was performed considering accuracy of digitization of strong motion records (Refs.2,3). The ground velocity and displacement were calculated by integrating the corrected acceleration in the frequency domain.

Two horizontal orthogonal components of the ground motion are combined on the horizontal plane. In case of acceleration records, an acceleration  $a^x(\theta, t)$  along the x-axis, which is arbitrarily rotated with an angle of  $\theta$  from the two horizontal axes X and Y representing the axes of the accelerograph, can be given as  $a^x(\theta, t) = a^X(t)\cos\theta + a^Y(t)\sin\theta$ . Representing  $a_{\max}(\theta)$  the peak value of  $a^x(\theta, t)$ , the maximum peak acceleration  $\tilde{a}_{\max}$  is defined as  $\tilde{a}_{\max} = \max\{a_{\max}(\theta)\}$  for  $\theta$ . Similarly, the maximum peak velocity  $\tilde{v}_{\max}$  and the maximum peak displacement  $\tilde{d}_{\max}$  can be defined.

Combination of the two horizontal components was also performed for absolute acceleration response spectra with 5% damping of critical, i.e., defining acceleration response spectrum for  $a^x(\theta, t)$  as  $S_A(\theta, T)$ , the maximum acceleration response spectrum on the horizontal plane can be obtained as  $\tilde{S}_A(T) = \max\{S_A(\theta, T)\}$  for  $\theta$ . Previous study showed that the maximum peak ground motions  $\tilde{a}_{\max}$ ,  $\tilde{v}_{\max}$  and  $\tilde{d}_{\max}$  determined by combination of two horizontal components are about 8% greater in magnitude than the larger of the two horizontal components (Ref.4). The study also showed that the maximum acceleration response spectra  $\tilde{S}_A(T)$  is about 15 to 20 greater in magnitude than the larger spectral amplitude between  $S_A^X$  and  $S_A^Y$ , in which  $S_A^X$  and  $S_A^Y$  represent acceleration response spectra calculated by  $a^X(t)$  and  $a^Y(t)$ , respectively.

#### ATTENUATION OF THE MAXIMUM PEAK GROUND MOTIONS

In determining attenuations of the maximum peak ground motions by multiple regression analysis, attenuation equations have to be properly selected. In the past analyses (Ref.5), the following empirical formula is often used

$$X(M, \Delta, GC_i) = a(GC_i) \times 10^{b(GC_i)M} \times (\Delta + 30)^{c(GC_i)} \quad (1)$$

in which,  $X(M, \Delta, GC_i)$  represents the maximum peak ground motions (acceleration  $\tilde{a}_{\max}$ [gal], velocity  $\tilde{v}_{\max}$ [cm/sec], and displacement  $\tilde{d}_{\max}$ [cm]) for a given magnitude of earthquake M, epicentral distance  $\Delta$ [km] and subsoil condition  $GC_i$  ( $i=1,2,3$ ). Coefficients  $a(GC_i)$ ,  $b(GC_i)$  and  $c(GC_i)$  are the constants to be determined for each subsoil condition. Although it is often claimed that M and  $\Delta$  are not necessarily suitable parameters to represent the magnitude of earthquake and the distance from source of energy released by earthquake for short period ground motions, they were used here because the magnitude (JMA magnitude) and the epicentral distance are the only parameters which can be definitely determined for all the earthquakes analyzed in this analysis.

Although all three coefficients a, b and c are assumed dependent on soil conditions in Eq.(1), the previous study showed that the differences of some coefficients, especially coefficient c, with respect to ground condition are

less significant (Ref.1). Therefore in order to examine the dependence of three coefficients on the ground conditions, eight types of attenuation equation as shown in Table 2 are considered, in which  $a(GC_i)$ ,  $b(GC_i)$  and  $c(GC_i)$  represent the coefficients which are dependent on soil conditions, and  $a$ ,  $b$  and  $c$  represent those which are independent of soil conditions. Although it is obvious that case-1 does not represent meaningful attenuation which takes account of soil conditions, it was analyzed for comparison with other cases.

Multiple regression analysis was performed for the maximum peak ground motions ( $\tilde{a}_{max}$ ,  $\tilde{v}_{max}$  and  $\tilde{d}_{max}$ ) with use of 197 sets of horizontal strong motion data, and accuracy of the eight empirical formulae for attenuation was examined in terms of correlation coefficient  $R$ . The adjusted correlation coefficient  $R^*$  defined by  $R^* = \sqrt{1-(n-1)/(n-p-1) \times (1-R^2)}$  is also used as an index of comparisons of accuracy, in which  $n$  and  $p$  represent the number of strong motion data and the number of terms considered in attenuation equations, respectively. Fig.1 shows  $R$  and  $R^*$  for eight attenuation equations, and it is observed from these results that  $R$  for case-2 to case-6 takes almost the same values and that  $R$  for case-7 and case-8 is a little larger than that for case-2 to case-6. The same characteristics are observed for comparisons in terms of  $R^*$  implying that the accuracy for case-7 and case-8 is appreciably higher than that of other cases. The coefficients  $a$ ,  $b$  and  $c$  for the both cases are shown in Table 3.

Because the accuracy of the attenuations in terms of  $R$  and  $R^*$  is almost the same between case-7 and case-8, actual attenuations of  $\tilde{a}_{max}$ ,  $\tilde{v}_{max}$  and  $\tilde{d}_{max}$  were computed for the earthquake magnitude of 6 and 8. Fig.2 shows an example of the attenuations thus calculated, and it is seen from Fig.2 that the difference of the predicted attenuation between case-7 and case-8 is rather small. It should be noted here that the effects of soil condition on the maximum peak acceleration seem insignificant although they are very apparent for the maximum peak velocity and displacement.

As seen from the correlation coefficients in Fig.1, correlations between the predicted values of the maximum peak ground motion and the observed values may be regarded as rather low. This implies that the observed values exhibit considerable deviation from the predicted values. The reason for such a large scatter is believed to be caused by insufficiency of the parameters assumed in the attenuation, i.e., although three principal parameters are selected for factors that may influence the peak ground motions, there are many other factors such as properties of path condition, focal mechanism, deeper site conditions, etc. It is therefore necessary to consider the scatter of the predicted value around the observed one when the above attenuations are to be used for practical purpose. For this purpose, ratios of the observed and predicted motions are defined as  $U_X = X^{OB}/X^P$  ( $X = \tilde{a}_{max}$ ,  $\tilde{v}_{max}$  and  $\tilde{d}_{max}$ ), in which superscript OB and P denote the observed and predicted values, respectively. The standard deviation of  $\log U_a$ ,  $\log U_v$  and  $\log U_d$  are shown in Table 4. The ratios  $U_a$ ,  $U_v$  and  $U_d$  are almost independent of earthquake magnitude and epicentral distance.

#### ATTENUATION OF ACCELERATION RESPONSE SPECTRUM

Absolute acceleration response spectral amplitude with damping ratio of 5% of critical corresponding to 10 discrete natural period  $T_k$  ( $k=1, 2, \dots, 10$ ) was assumed to be represented in terms of earthquake magnitude  $M$  and epicentral distance  $\Delta$  [km] for three soil conditions as

$$\tilde{S}_A(T_k, M, \Delta, GC_i) = a(T_k, GC_i) \times 10^{b(T_k, GC_i)M} \times (\Delta + 30)^{c(T_k, GC_i)} \quad (2)$$

in which coefficients  $a(T_k, GC_i)$ ,  $b(T_k, GC_i)$  and  $c(T_k, GC_i)$  are the constants

to be determined by multiple regression analysis for each natural period  $T_k$  and soil condition  $GC_i$ .

As is the case of the maximum peak ground motions, dependence of the coefficients  $a$ ,  $b$  and  $c$  on the soil conditions  $GC_i$  ( $i=1,2,3$ ) together with the dependence of the coefficients on the natural periods  $T_k$  ( $k=1, 2, \dots, 10$ ) was examined through the same procedure described in the preceding section. For this purpose, multiple regression analysis was performed assuming the empirical formulae of attenuation as shown in Tables 5 and 6, in which coefficients  $f(T_k, GC_i)$ ,  $f(T_k)$  and  $f(GC_i)$  ( $f=a, b$  and  $c$ ) represent the coefficients which are dependent on both natural period  $T_k$  and soil condition  $GC_i$ , natural period  $T_k$ , and soil conditions  $GC_i$ , respectively. It should be noted that the attenuation equation of case-8 in Table 5 is the same with that of case-8 in Table 6, and that although attenuation equations of case-1 in both Tables 5 and 6 are meaningless to represent response spectral values which change in accordance with  $T_k$  and  $GC_i$ , they were analyzed only for comparison with other cases.

Figs.3 and 4 show the dependence of coefficients  $a$ ,  $b$  and  $c$  on soil conditions and the dependence of the same coefficients on natural period, respectively. Only the results for natural period of 0.5 sec and 1.5 sec are presented in Fig.3 because the results for other natural periods are of the same type. It is seen from Figs.3 and 4 that the correlation coefficient  $R$  as well as the adjusted correlation coefficient  $R^*$  takes the highest value at case-7 and case-8. Consequently the following 4 formulae may be regarded as the most suitable equations to represent the attenuation of the response spectral amplitudes corresponding to the natural period of 0.1 and 3 seconds.

$$\tilde{S}_A(T_k, M, \Delta, GC_i) = a(T_k, GC_i) \times 10^{b(T_k, GC_i)M} \times (\Delta + 30)^{c(T_k, GC_i)} \quad (3)$$

$$\tilde{S}_A(T_k, M, \Delta, GC_i) = a(T_k, GC_i) \times 10^{b(T_k, GC_i)M} \times (\Delta + 30)^{c(T_k)} \quad (4)$$

$$\tilde{S}_A(T_k, M, \Delta, GC_i) = a(T_k, GC_i) \times 10^{b(T_k, GC_i)M} \times (\Delta + 30)^{c(GC_i)} \quad (5)$$

$$\tilde{S}_A(T_k, M, \Delta, GC_i) = a(T_k, GC_i) \times 10^{b(T_k, GC_i)M} \times (\Delta + 30)^c \quad (6)$$

Eqs.(3), (4) and (5) correspond to case-8 of Table 5 (= case-8 of Table 6), case-7 of Table 5, case-7 of Table 6, respectively. Eq.(6) was obtained by combining Eqs.(4) and (5). Because the general trend of the four formulae are of the same type, concentration is placed on the comparisons between Eq. (3) and Eq.(6).

Figs.5 and 6 show the variation of coefficients  $a$ ,  $b$  and  $c$  with respect to natural period for three soil conditions (coefficients of Eq.(6) are shown in Table 7). It is seen that the coefficients  $a$  and  $b$  change in accordance with natural period in a similar manner between Eq.(3) and Eq.(6). The coefficient  $c$  of Eq.(3) takes a value from -0.8 to -1.7 depending on natural period and soil condition, whereas consistent variation of  $c$  in accordance with natural period is not observed for any ground conditions. The coefficient  $c$  of Eq.(5) is equal to -1.24, -1.14 and -1.19 for ground group of 1, 2 and 3, respectively, showing that the difference of  $c$  between three ground conditions is less than 0.1. It gives credit to use the same value for  $c$  in Eq.(6), in which the coefficient  $c$  is equal to -1.18.

Fig.7 shows comparisons of response spectra between Eq.(3) and Eq.(6) for combination of earthquake magnitude of 6, 7 and 8, and epicentral distance of 50 km for three soil conditions. The two empirical formulae predict almost the same spectral values excluding the combination of large magnitude of earthquake and short epicentral distance. It should be noted here that both empirical formulae for attenuation should not directly be used for such combination

of earthquake magnitude and epicentral distance because strong motion data corresponding to such conditions are not include in this analysis. Although Eqs.(3) ~ (6) gives the similar attenuation of spectral amplitude excluding the extreme combinations of earthquake magnitude and epicentral distance, Eq.(6) is proposed here among the four formulae considering that the coefficients are the most simple in number and that the response spectral amplitude predicted changes realistically in accordance with natural period.

As is the case of the maximum peak ground motion, correlations between predicted and observed values of spectral amplitude are not necessarily high. To investigate the scatter of the observed values around the predicted ones, ratios of observed (OB) and predicted (P) spectral amplitudes are defined as  $U_{SA}(T) = \tilde{S}_A^{OB}(T)/\tilde{S}_A^P(T)$ . Standard deviation of  $\log U_{SA}(T)$  is shown in Table 8.

Finally, the response spectral amplitude  $\tilde{S}_A(T, h)$  of arbitrary damping ratio  $h$  may be obtained from the response spectral amplitude  $\tilde{S}_A(T, 0.05)$  of 5% damping of critical as (Ref. 6)

$$\tilde{S}_A(T, h) = \tilde{S}_A(T, 0.05) \times \left\{ \frac{1.5}{40h+1} + 0.5 \right\} \times \beta(T, 0.05)^{\left\{ \frac{1}{300h+6} - 0.8h \right\}} \quad (7)$$

in which  $\beta(T, 0.05)$  represents acceleration response spectral ratio ( $=\tilde{S}_A(T, 0.05)/\tilde{a}_{max}$ ) of 5% damping. When the value of  $\beta(T, 0.05)$  is close to 1.0, the third term may be dropped out without introducing serious error.

#### CONCLUSIONS

The preceding pages present the results of a study of multiple regression analysis of peak ground motions and absolute acceleration response spectra with 5% damping of critical. Attenuations of these characteristics in terms of earthquake magnitude and epicentral distances are proposed for three sub-soil conditions. In this analysis, combination of two horizontal orthogonal components were considered, and instrumentally corrected Japanese data were used. The results might be expected to provide a realistic basis for assessing the characteristics of earthquake ground motions for wide range of soil conditions.

#### REFERENCE

- 1) Okubo, T., Arakawa, T. and Kawashima, K.: Attenuation of Peak Ground Motions and Absolute Acceleration Response Spectra with Use of Japanese Strong Motion Data, International Symposium on Lifeline Earthquake Engineering on Pressure Vessels and Piping Technology, ASME, Portland Oregon, U.S.A, 1983
- 2) Kawashima, K., Takagi, Y. and Aizawa, K.: Procedure of Instrument Correction and Displacement Calculation for SMAC-B2 Accelerograph Records with Considering Accuracy of Digitization, Proc. of Japan Society of Civil Engineers (JSCE), No.325, 1982.
- 3) Kawashima, K., Takagi, Y. and Aizawa, K.: Accuracy of Digitization of Strong Motion Records obtained by SMAC-Accelerograph, Proc. of JSCE, No. 323, 1982
- 4) Kawashima, K., Aizawa, K. and Takahashi, K.: Effects of Composition of Two Horizontal Components on Attenuation of Maximum Earthquake Ground Motions and Response Spectra, Proc. of JSCE, No. 329, 1983
- 5) Idriss, I. M.: Characteristics of Earthquake Ground Motions, State-of-the-Arts Report, Earthquake Engineering and Soil Dynamics, Proc. of ASCE Geotechnical Engineering Division Speciality Conference, 1978
- 6) Kawashima, K., Aizawa, K. and Takahashi, K.: Effects of Damping Ratio on Earthquake Response Spectra, Proc. JSCE, No.335, 1983

Table-1 Classification of Ground Conditions

Soil Condition in this Analysis	Classification of Highway Bridge Specifications			Alternative Approach when Precise Soil Data are not available
	Soil Condition	Geological Definition	Definition by Natural Period	
Group-1	Group-1	Tertiary or older rock (defined as bed-rock), or diluvium with $H < 10$ m	$T_0 < 0.2$ sec	$\beta(0.7) < 0.7$
Group-2	Group-2	Diluvium with $H \geq 10$ m, or alluvium with $H < 10$ m	$0.2 < T_0 < 0.4$ sec	$0.7 \leq \beta(0.7) \leq 1.8$
	Group-3	Alluvium with $H < 25$ m including soft layer with thickness less than 5 m	$0.4 < T_0 < 0.6$ sec	
Group-3	Group-4	Other than the above, usually soft alluvium or reclaimed land	$T_0 > 0.6$ sec	$\beta(0.7) > 1.8$

Table-2 Attenuation Formulae of Peak Ground Motions ( $x = \tilde{a}_{\max}$ ,  $\tilde{v}_{\max}$  and  $\tilde{d}_{\max}$ )

CASE	ATTENUATION EQUATION
1	$a \times 10^{bM} \times (\Delta + 30)^c$
2	$a \times 10^{bM} \times (\Delta + 30)^{c(GC_i)}$
3	$a \times 10^{b(GC_i)M} \times (\Delta + 30)^c$
4	$a(GC_i) \times 10^{bM} \times (\Delta + 30)^c$
5	$a \times 10^{b(GC_i)M} \times (\Delta + 30)^{c(GC_i)}$
6	$a(GC_i) \times 10^{bM} \times (\Delta + 30)^{c(GC_i)}$
7	$a(GC_i) \times 10^{b(GC_i)M} \times (\Delta + 30)^c$
8	$a(GC_i) \times 10^{b(GC_i)M} \times (\Delta + 30)^{c(GC_i)}$

Table-4 Standard Deviation of  $\log U_a$ ,  $\log U_v$  and  $\log U_d$ 

	GROUP 1	GROUP 2	GROUP 3
$\log U_a$	0.216	0.224	0.197
$\log U_v$	0.236	0.239	0.243
$\log U_d$	0.262	0.258	0.262

Table-3 Coefficient a, b and c of Eq.(1) for Cases-7 and 8 in Table-2

TYPE	GROUND GROUP	CASE-7			CASE-8		
		a	b	c	a	b	c
$\tilde{a}_{\max}$	1	987.4	0.216	-1.218	1073	0.221	-1.251
	2	232.5	0.313		222.7	0.308	-1.201
	3	403.8	0.265		403.1	0.262	-1.208
$\tilde{v}_{\max}$	1	20.8	0.263	-1.222	23.9	0.271	-1.275
	2	2.81	0.430		2.67	0.421	-1.183
	3	5.11	0.404		5.14	0.415	-1.257
$\tilde{d}_{\max}$	1	0.626	0.372	-1.254	0.886	0.393	-1.390
	2	0.062	0.567		0.056	0.549	-1.179
	3	0.070	0.584		0.070	0.575	-1.224

Table-8 Standard Deviation of  $\log U_{SA}$ 

GROUND CONDITION	T=0.1 s.	T=0.15 s.	T=0.2 s.	T=0.3 s.	T=0.5 s.	T=0.7 s.	T=1 s.	T=1.5 s.	T=2 s.	T=3 s.
GROUP 1	0.262	0.229	0.226	0.241	0.278	0.239	0.273	0.254	0.267	0.249
GROUP 2	0.256	0.244	0.273	0.270	0.249	0.245	0.305	0.288	0.264	0.248
GROUP 3	0.219	0.218	0.211	0.217	0.240	0.243	0.307	0.305	0.276	0.263

Table-5 Attenuation Formulae of Acceleration Response Spectral Amplitude for Examination of Dependence of Coefficients a, b and c on Soil Conditions

CASE	ATTENUATION EQUATION
1	$a(T_k) \times 10^{b(T_k)H} \times (\Delta + 30)^c(T_k)$
2	$a(T_k) \times 10^{b(T_k)H} \times (\Delta + 30)^c(T_k, GC_1)$
3	$a(T_k) \times 10^{b(T_k, GC_1)H} \times (\Delta + 30)^c(T_k)$
4	$a(T_k, GC_1) \times 10^{b(T_k)H} \times (\Delta + 30)^c(T_k)$
5	$a(T_k) \times 10^{b(T_k, GC_1)H} \times (\Delta + 30)^c(T_k, GC_1)$
6	$a(T_k, GC_1) \times 10^{b(T_k)H} \times (\Delta + 30)^c(T_k, GC_1)$
7	$a(T_k, GC_1) \times 10^{b(T_k, GC_1)H} \times (\Delta + 30)^c(T_k)$
8	$a(T_k, GC_1) \times 10^{b(T_k, GC_1)H} \times (\Delta + 30)^c(T_k, GC_1)$

Table-6 Attenuation Formulae of Acceleration Response Spectral Amplitude for Examination of Dependence of Coefficients a, b and c on Natural Period

CASE	ATTENUATION EQUATION
1	$a(GC_1) \times 10^{b(GC_1)H} \times (\Delta + 30)^c(GC_1)$
2	$a(GC_1) \times 10^{b(GC_1)H} \times (\Delta + 30)^c(T_k, GC_1)$
3	$a(GC_1) \times 10^{b(T_k, GC_1)H} \times (\Delta + 30)^c(GC_1)$
4	$a(T_k, GC_1) \times 10^{b(GC_1)H} \times (\Delta + 30)^c(GC_1)$
5	$a(GC_1) \times 10^{b(T_k, GC_1)H} \times (\Delta + 30)^c(T_k, GC_1)$
6	$a(T_k, GC_1) \times 10^{b(GC_1)H} \times (\Delta + 30)^c(T_k, GC_1)$
7	$a(T_k, GC_1) \times 10^{b(T_k, GC_1)H} \times (\Delta + 30)^c(GC_1)$
8	$a(T_k, GC_1) \times 10^{b(T_k, GC_1)H} \times (\Delta + 30)^c(T_k, GC_1)$

Table-7 Coefficients a, b and c of Eq.(6)

NATURAL PERIOD T [SEC]	GROUND GROUP 1		GROUND GROUP 2		GROUND GROUP 3	
	a(T <sub>k</sub> , GC <sub>1</sub> )	b(T <sub>k</sub> , GC <sub>1</sub> )	a(T <sub>k</sub> , GC <sub>1</sub> )	b(T <sub>k</sub> , GC <sub>1</sub> )	a(T <sub>k</sub> , GC <sub>1</sub> )	b(T <sub>k</sub> , GC <sub>1</sub> )
0.1	2420	0.211	848.0	0.262	1307	0.208
0.15	2407	0.216	629.1	0.288	948.2	0.238
0.2	1269	0.247	466.0	0.315	1128	0.228
0.3	574.8	0.273	266.8	0.345	1263	0.224
0.5	211.8	0.299	102.2	0.388	580.6	0.281
0.7	102.5	0.317	34.34	0.440	65.67	0.421
1.0	40.10	0.344	5.04	0.548	7.41	0.541
1.5	7.12	0.432	0.719	0.630	0.803	0.647
2.0	5.78	0.417	0.347	0.644	0.351	0.666
3.0	1.67	0.462	0.361	0.586	0.262	0.635

c = -1.178

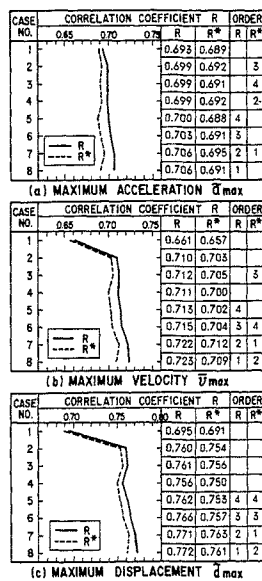


Fig.1 Examination of Dependence of Coefficients a, b and c on Soil Conditions

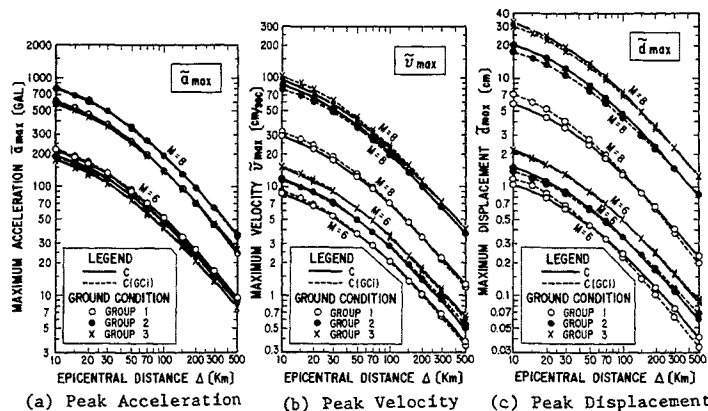
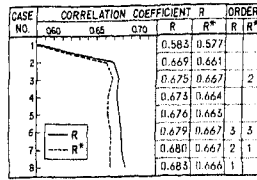
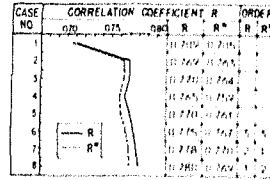


Fig.2 Comparisons of Empirical Formulae between Case-7 and Case-8

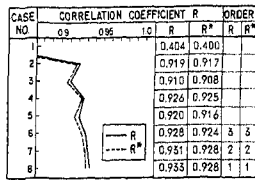


(a)  $T = 0.5$  sec

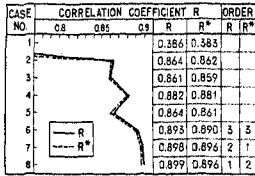


(b)  $T = 1.5$  sec

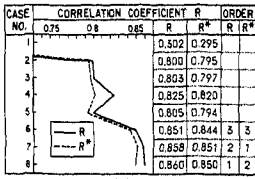
Fig.3 Examination of Dependence of Coefficients a, b and c on Soil Conditions



(a) GROUND GROUP 1

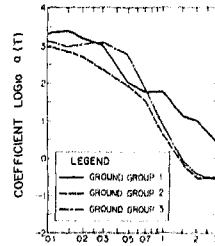


(b) GROUND GROUP 2

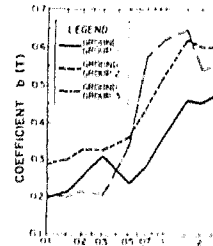


(c) GROUND GROUP 3

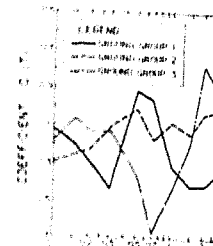
Fig.4 Examination of Dependence of Coefficients a, b and c on Natural Period



(a) Coefficient a

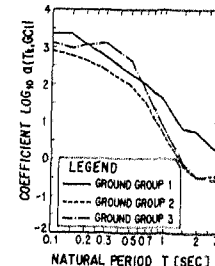


(b) Coefficient b

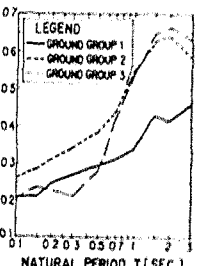


(c) Coefficient c

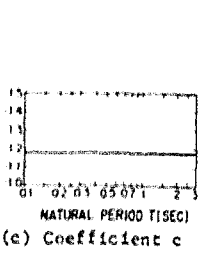
Fig.5 Coefficients a, b and c of Eq.(3)



(a) Coefficient a



(b) Coefficient b



(c) Coefficient c

Fig.6 Coefficients a, b and c of Eq.(6)

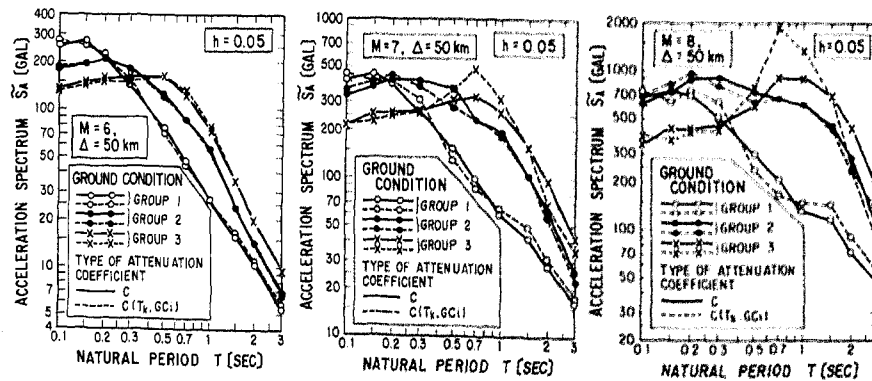


Fig.7 Comparison of Response Spectra Predicted by Eq.(3) and Eq.(6)